Heat Mass Transfer (2009) 46:267–275
DOI 10.1007/s00231-009-0563-0

ORIGINAL

Operational characteristics of miniature loop heat pipe with flat evaporator

Dongxing Gai · Zhichun Liu · Wei Liu · Jinguo Yang

Received: 19 June 2009 / Accepted: 15 November 2009 / Published online: 5 December 2009

Abstract Loop heat pipes are heat transfer devices whose operating principle is based on the evaporation and condensation of a working fluid, and which use the capillary pumping forces to ensure the fluid circulation. A series of tests have been carried out with a miniature loop heat pipe (mLHP) with flat evaporator and fin-and-tube type condenser. The loop is made of pure copper with stainless mesh wick and methanol as the working fluid. Detailed study is conducted on the start-up reliability of the mLHP at high as well as low heat loads. During the testing of mLHP under step power cycles, the thermal response presented by the loop to achieve steady state is very short. At low heat loads, temperature oscillations are observed throughout the loop. The amplitudes and frequencies of these fluctuations are large at evaporator wall and evaporator inlet. It is expected that the extent and nature of the oscillations occurrence is dependent on the thermal and hydrodynamic conditions inside the compensation chamber. The thermal resistance of the mLHP lies between 0.29 and 3.2°C/W. The effects of different liquid charging ratios and the tilt angles to the start-up and the temperature oscillation are studied in detail.

List of symbols

A	Area (m^2)
Q	Heat load (W)
R	Thermal resistance (°C W^{-1})
T	Temperature (°C)
cond	Condenser
cond-fin	Fin of condenser
cond-in	Condenser inlet
cond-out	Condenser outlet
evap	Evaporator
evap-in	Evaporator inlet
evap-out	Evaporator outlet
evap-wall	Active zone of evaporator
air	Ambient air

Greek symbols

λ	Thermal conductivity (W m^{-1} k^{-1})
θ	Tilt angle, degree (°)

D. Gai (✉) · Z. Liu · W. Liu · J. Yang
School of Energy and Power Engineering, Huazhong University of Science and Technology, Wuhan, Hubei, China
e-mail: gaidongxing@smail.hust.edu.cn

1 Introduction

A loop heat pipe is a highly efficient heat-transfer device which does not require any additional regulating actions from the outside for ensuring its serviceability. Thus, LHPs offer many advantages over traditional heat exchanger, such as operability against gravity, over large distance with minimal temperature loss and no moving parts for pumping the working fluid, etc. A detailed review of the main characteristics of LHPs can be found in [1, 2]. LHPs have been successfully used in space engineering. With increasing power densities of electric devices, the LHP technology continues to be an important area of research. The mLHP with the cylindrical as well as flat evaporators have been developed and tested successfully. Compared with conventional cylindrical LHPs, the LHPs with flat evaporator have more advantages: firstly, it is more convenient for the flat-plate type evaporator to connect with the electronic devices which should be cooled, because most objects to be cooled have a flat thermal contact surface; secondly, the angle of velocity grads and temperature gradient is smaller than that of LHPs with cylindrical

evaporator, from the viewpoint of field synergy principle, the heat transfer efficiency of flat evaporator is better [3]. So the capability of LHP with flat-plate evaporator for transferring high heat-flux achieve easily. The LHPs with flat evaporator can be considered as an optimum design for compact enclosures as it provide relatively more scope for design miniaturization.

LHPs provide a unique way for transporting heat using phase change. The structure of LHPs can be various in terms of size, geometric shape, relative position, material, working fluid, charging ratio, etc. The performance characteristics of LHPs are very complicated, the main objective of the present study is to design and investigate the start-up phenomenon, steady state performance, operating characteristic at variable heat load cycles and temperature oscillation phenomenon of the flat evaporator miniature loop heat pipe with copper body, stainless mesh wick and methanol as working fluid. The thermal oscillations are characterized by the continuous fluctuations in the temperature at different locations of mLHP and thus inability of the evaporator to attain stable operating conditions. These oscillations are expected to result from the thermal and hydrodynamic interaction between the compensation chamber, condenser and evaporator section [4, 5]. Copper-stainless steel–methanol combination is chosen for the present investigation due to the viability and acceptability of such a system for electronic cooling applications. The present research also endeavors to test the compatibility of the copper-stainless steel-methanol system for loop heat pipe applications.

2 Experimental prototype and test procedure

An experimental prototype of miniature LHP as shown in Fig. 1 is constructed for carrying out the present investigation (Appendix). The overall system is made up of evaporator with porous wick, vapor line, fin-tube condenser and liquid line. The evaporator was made in the shape of the flat rectangle with the active zone 40 × 30 mm and thickness of 13.5 mm. There are 15 longitudinal and 18 latitudinal grooves machined on the inside of the evaporator active heated zone which behave as vapor removal channels and also provide heat to the skeleton of the porous structure through conduction process. The evaporator is made from pure copper that provide superior thermal conductivity and minimal heat spreading resistance from the source to the porous wick surface. The Fig. 1b illustrates the cross section of the evaporator assembly showing the location of the vapor channels, wick structure and compensation chamber. The porous wick of evaporator is 4 mm thickness, which is made up of 82 layers 500 grids stainless steel mesh. The compensation chamber is 6 mm thickness, which acts as a liquid reservoir and accommodates the extra liquid inventory displace from the other parts of the loop during start-up and transient operating

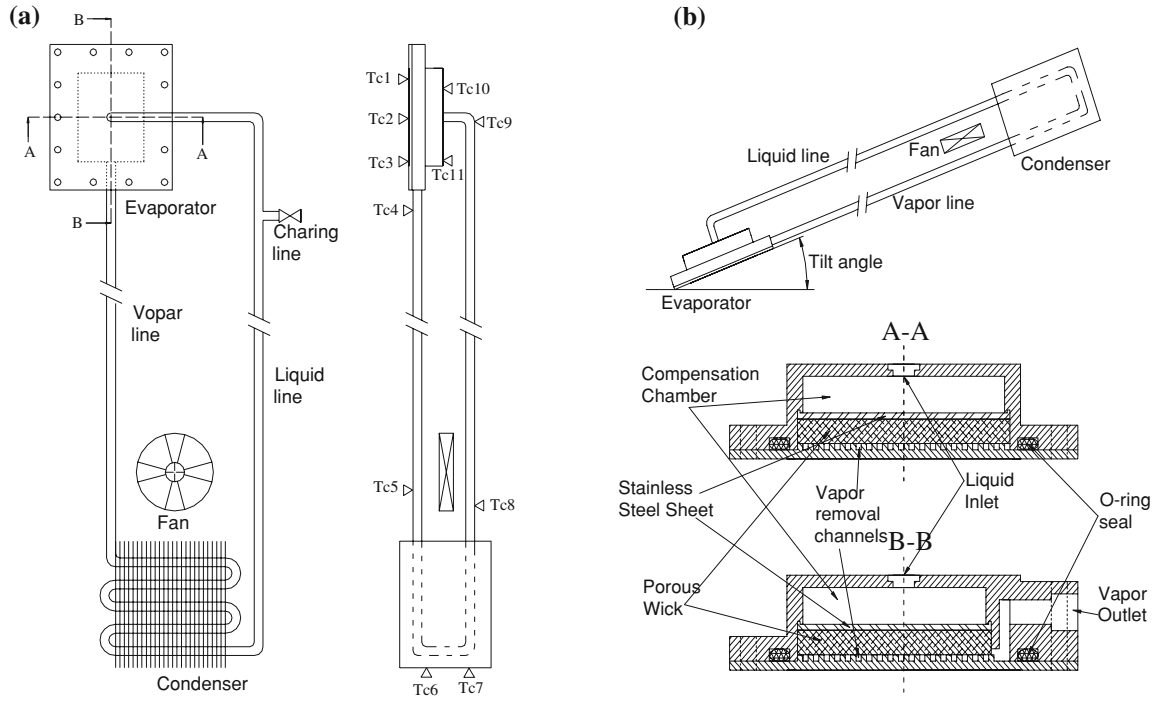

Fig. 1 Schematics of the mLHP. **a** Top and side view of the mLHP and the placement of the thermocouple points. **b** Cross section of the mLHP evaporator

Table 1 Geometric characteristics of the experimental mLHP

Evaporator	
Active heated zone	
Thickness (mm)	1.5
Length/width (mm)	40/30
Groove thickness (mm)	1
Fin width (mm)	1 × 1
Fin number	18 × 15
Wall	
Thickness (mm)	1.5
Stainless steel sheet	
Thickness (mm)	0.5
Compensation chamber	
Length/width (mm)	34.5/30
Height (mm)	6
Porous wick	
Length/width/height (mm)	36.5/30/4
Material	316L
Parameter of mesh	500#, 82 layers
Vapor line	
Diameter(O/I) (mm)	6/4
Length (mm)	320
Liquid line	
Diameter(O/I) (mm)	6/4
Length (mm)	530
Condenser	
Diameter(O/I) (mm)	6/4
Length (mm)	810
Fin thickness (mm)	0.05
Fin length/width (mm)	100/20
Fan rotate speed (rpm)	3,000

conditions. There is a stainless steel sheet with grooves between the porous wick and the compensation chamber to sustain the stainless steel wick. The geometric characteristics of the experimental mLHP are shown in Table 1.

The mLHP condenser is fin-and-tube type with the total tube length of 810 mm and cross section of 100 × 20 mm for each fin. A centrifugal fan is used to dissipate heat from the condenser to the ambient by means of forced convection of air with temperature of 20 ± 2°C. The vapor line of the mLHP is 320 mm in length and 4 mm internal diameter. For the return of the condensate to the evaporator, a liquid return line with the total length of 530 and 4 mm internal diameter is used. The transport lines and the condenser fin are overall made from pure copper. The mLHP is hermetically sealed by an O-ring seal between the evaporator flanges. For charging, the loop is firstly evacuated to 3.2×10^{-4} Pa and then filled with the predetermined quantity of methanol whose purity is 99.5%. In order to test the thermal performance of the mLHP, a heat load simulator in the form of copper block with two embedded cartridge heater and active area of 40 × 30 mm is used, which is uniform to the evaporator. For the purpose of minimizing heat losses to the ambient, the heat load simulator is thermally insulated using 10 mm thickness nano-adiabatic material whose conductivity is just 0.012 W/m K. The temperatures of two sides of the heat insulation have been measured during the experiments. According to Fourier's law of heat conduction: $Q_{\text{loss}} = -\lambda A \Delta T/b$, the quantity of heat loss is 0.28 W as the heat load attains the largest 120 W. So the head load simulator needn't equalize, and the absolute error of the heat load is less than 0.3%. The other parts of the mLHP are not heat preservation except the heat load simulator and the active surface of evaporator.

A digital power meter with accuracy of ±0.2 W was used to measure and control the input power to the heat load simulator. Twelve T-type thermocouples with ±0.2°C accuracy are used to measure the temperature at different locations of the mLHP and the ambient air. Figure 1 also shows the placement of the thermocouple points. All the instruments are connected to the Keyence Thermo Pro 2700 data acquisition system which helps to monitor and record the test data from the mLHP prototype at a time interval of every 1.5 s.

In this phase of experiments, the mLHP is operated at the tilt angle (θ) of 10, 50 and 90°, and the charging ratio of 50, 60 and 70 vol.% in the cold mode. The procedure of tests included measurements of temperatures at characteristic points of the mLHP with a successive stepwise 12 W increase and decrease of the heat load. And the heat loads of start-up tests are from 12 W (heat-flux density 1 W/cm^2) to 120 W (heat-flux density 10 W/cm^2). For the safety of tests the maximum heat-load is limited by the value that the evaporator wall operating temperature reaches 75°C.

3 Result and discussion

3.1 Thermal resistance

Thermal resistance offered by the mLHP (R_{mLHP}) from evaporator to condenser external surface is used to access the heat transfer performance of the device. R_{mLHP} is calculated as:

$$R_{\text{mLHP}} = (T_{\text{evap}} - T_{\text{cond}})/Q$$

where, T_{evap} is the external temperature of the evaporator active zone which is measured by taking mean of the temperatures from the thermocouples fixed on the evaporator external surface ($T_{\text{evap-wall}}$); T_{cond} is the condenser temperature calculated by averaging the readings from the condenser inlet temperature ($T_{\text{cond-in}}$), condenser fin

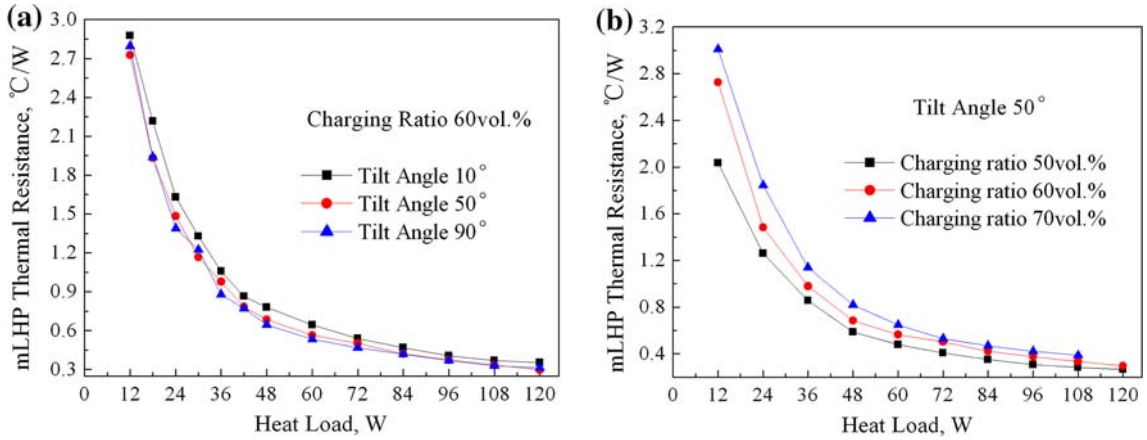

Fig. 2 Thermal resistance at different heat loads

temperatures ($T_{\text{cond-fin}}$) and condenser outlet temperature ($T_{\text{cond-out}}$); Q is the applied heat load.

It is observed in Fig. 2 that the thermal resistance decreases with the heat load increasing. Figure 2a shows the effect of tilt angle to the thermal resistance of the mLHP, it indicates that increasing the tilt angle could decrease the thermal resistance at the same heat load. The R_{mLHP} at 90°–60 vol.% operation condition is average smaller 13.85% than that of 10°–60 vol.% operation condition. The reason is that the condenser temperature is almost equal as long as the applied heat load is same, but the evaporator temperature is concerned to the tilt angle. The mLHP at bigger tilt angle could utilize gravity to push the working fluid into the compensation chamber, which increases the thermal capacity of the evaporator, otherwise, there is less force to drive the system for the less working fluid in the condenser and the larger gravity used, which decreases the vapor pressure. The less vapor pressure means lower vapor temperature and evaporator external surface temperature.

Figure 2b presents the thermal resistance of mLHP at different charging ratios, different heat loads and the same tilt angle. It indicates that the thermal resistance of the mLHP is greatly influenced by the fluid charging ratio. The thermal resistance decreases with decreasing the charging ratio. In the same condition of 50° tilt angle, the thermal resistance of 70 vol.% charging ratio is average larger 37.45% than that of 50 vol.% charging ratio at different heat loads. The reason is that the mLHP need larger vapor pressure to drive the loop for the larger quality of working fluid at larger charging ratio. The larger vapor pressure means the higher vapor temperature and evaporator external surface temperature, but the condenser temperature is almost equal at the same heat load.

On the basis of analysis above, the thermal resistance of the mLHP decreases with increasing the heat load, increasing the tilt angle and deceasing the charging ratio. The thermal resistance of the mLHP lies between 0.29 and 3.2°C/W in all conditions.

3.2 Start-up tests

The start-up performance is very critical in evaluating the reliability of the mLHP. Figure 3a–d respectively show the start-up of the mLHP at heat loads of 12, 30, 60 and 120 W in the condition of 50° tilt angle and 50 vol.% charging ratio. It is clear from the start-up trends that the mLHP is able to achieve steady state conditions at both low and high heat loads. The start-up profiles demonstrated by the loop for different heat loads are more or less similar except that the start-up time and temperature. From the comparison of the start-up profiles, the start-up performance of mLHP contains three main processes as shown in Fig. 3a–d: (I) clearing off the liquid from evaporator grooves, vapor line and part of condenser, the I-zone is the first part of the start-up time; and (II) generating enough pressure difference across the porous wick that is necessary to drive the working fluid around the loop, the II-zone is the second part of the start-up time; (III) the mLHP system achieve steady state or temperature oscillation state. For the loop, the start-up time is the actual time required to accomplish these processes. The first condition is achieved by the vapor generation inside the evaporator which helps to push liquid from grooves, vapor line and portion of condenser to the compensation chamber. It is shown in curve that the time from start to $T_{\text{evap-in}}$ fallen to the first low peak. In order to realize the second condition, steady temperature difference across the porous wick is necessary. The temperature gradient across the porous wick depends on hydraulic losses inside loop except porous wick, thermal characteristics of wick and hydrodynamic conditions inside compensation chamber which includes vapor fraction, parasitic heat load from evaporator, subcooled liquid flow rate from condenser and the heat loss to ambient air. It is

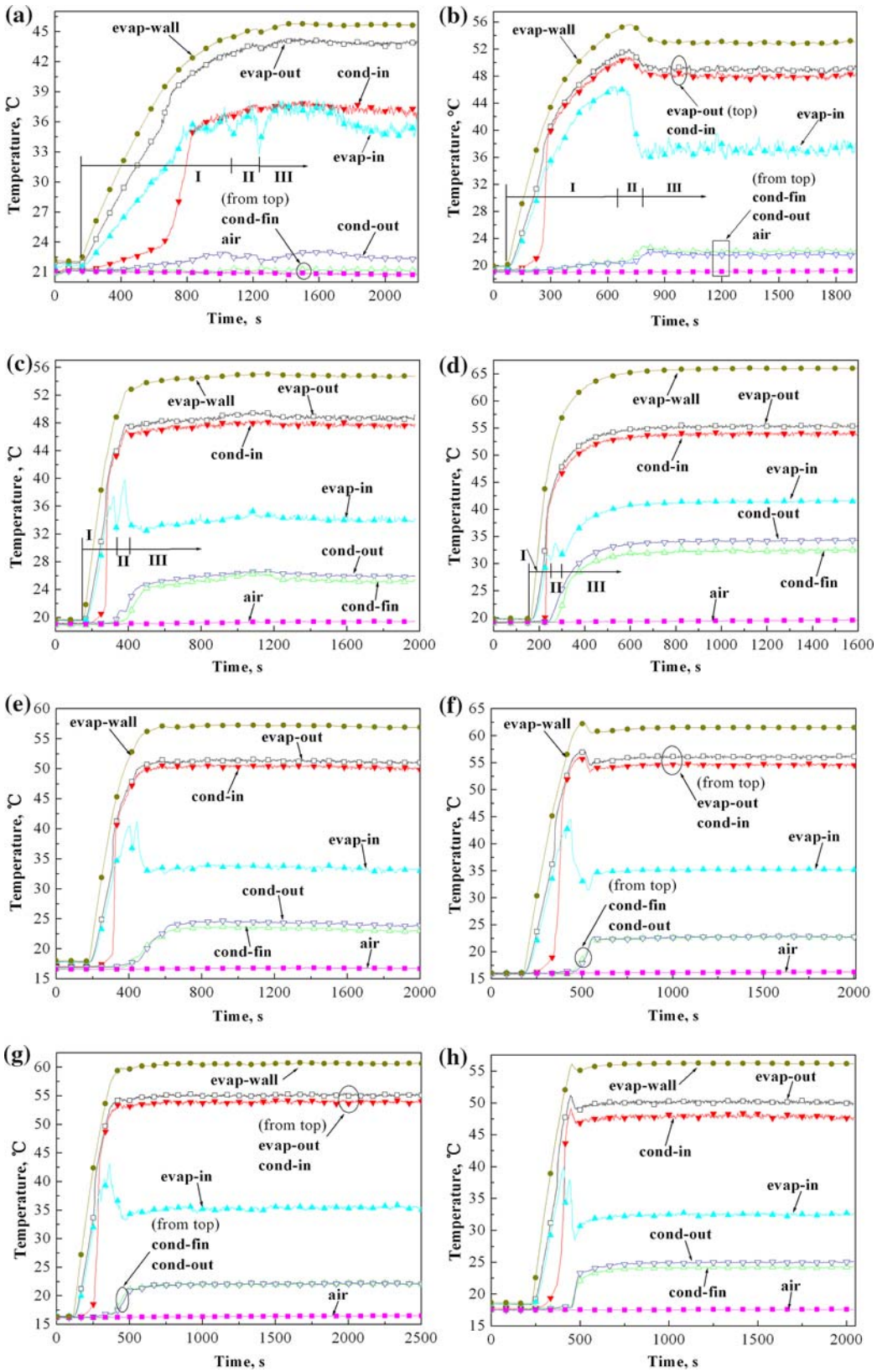

Fig. 3 Start-up of the mLHP. **a** $\theta = 50°$, 50 vol.%, $Q = 12$ W. **b** $\theta = 50°$, 50 vol.%, $Q = 36$ W. **c** $\theta = 50°$, 50 vol.%, $Q = 60$ W. **d** $\theta = 50°$, 50 vol.%, $Q = 120$ W. **e** $\theta = 50°$, 60 vol.%, $Q = 60$ W. **f** $\theta = 50°$, 70 vol.%, $Q = 60$ W. **g** $\theta = 10°$, 60 vol.%, $Q = 60$ W. **h** $\theta = 90°$, 60 vol.%, $Q = 60$ W

shown in curve that the time from $T_{evap\text{-}in}$ fallen to the first low peak to the second one. It is noted that completion of the first condition must to lay grounds for satisfying the second condition. After the start-up, the loop temperatures adjust themselves to a steady state or to a periodically oscillating state.

3.2.1 *Effect of power load to start-up*

Figure 3a–d present the start-up of the mLHP at 50° tilt angle, 50 vol.%, and the heat load of 12, 36, 60 and 120 W respectively. The temperature of evaporator increases with the heat load increase. It is obvious that the I-zone and II-zone of start-up time decrease with the heat load increasing. At low heat load, the vapor generation process inside the evaporation zone is slower than that at high heat load, which increases the start-up time. The results of start-up show that the mLHP could achieve steady state in different heat load.

3.2.2 *Effect of fluid charge to start-up*

The charging ratio of the liquid inside the loop plays an important part in prevention the start-up failure of the mLHP device. It was experimentally observed in [6] that liquid charging ratio from 50 to 80 vol.% was acceptable for the reliable start-up and steady state operation of the loop. For lower charge (<50%), there are consequences of wick dry out due to inadequate liquid inside the compensation chamber where for higher charge (>80%), the active condenser area is not sufficient for heat removal. Figure 3c–f present the start-up of the mLHP at heat load of 60 W, 50° tilt angle and 50, 60, 70 vol.% charging ratios, respectively. It is clear that the condenser temperatures are almost equal, but $T_{evap\text{-}out} - 70$ vol.% $> T_{evap\text{-}out} - 60$ vol.% $> T_{evap\text{-}out} - 50$ vol.%. The reason is that the mLHP need larger vapor pressure to circulate the loop for the larger quality of working fluid at larger charging ratio, so the evaporator temperatures of larger charging ratio are higher than those of less charging ratio condition. There is a little superheating before reaching steady state in Fig. 3f. The reason is that the second process of start-up needs larger pressure difference to drive the loop which increases the superheat of vapor. The experimental results indicate that the start-up time of less charging ratio is shorter than that of larger charging ratio.

3.2.3 *Effect of tilt angle to start-up*

In the gravity environment, a tilt modification will change the working fluid distribution, especially inside the compensation chamber and the evaporator core. Figure 3e–h show the start-up of the mLHP at heat load 60 W, 60 vol.% charging ratio and 50, 10, 90° tilt angles, respectively. The temperature of the evaporator decreases with the increase of tilt angle. The reason is that the system could utilize more gravity to drive the cycle, which decreases the pressure difference of the cycle and the saturation temperature of evaporation. Moreover, the tilt angle modification changes the start-up time of the mLHP. It is noted that the start-up time decreases with the tilt angle increase. The reason is that the saturation temperature decrease for the increase of tilt angle, which shorten the I-zone time, and the pressure difference across the wick decreases due to gravitational head, which shorten the II-zone of start-up time. So the larger tilt angle is useful for start-up of mLHP.

3.3 Temperature oscillation

Temperature oscillation is a rather wide-spread phenomenon accompanying the mLHP operation. The investigations conducted make it possible to differentiate three main types of the LHP operating temperature [7–13]. The first of them is characterized by a low-amplitude (no more than 1°C) and a high-frequency; The second type is also characterized by a low-amplitude (no more than several centigrade) of temperature oscillation, but their cycle is longer and reaches several minutes; The third type is distinguished by high amplitude of temperature oscillation, which reaches tens of degrees, and a still longer period, which may be equal to tens of minutes.

The Fig. 4 shows the temperature oscillation of the mLHP at some operation conditions. It is shown the periods are same and the amplitudes are different at each zones of mLHP. It is experimentally observed that the temperature oscillation is relative to the applied heat load, title angle and charging ratio. In general, the temperature oscillation phenomenon occurs at low heat load, it disappear when the heat load is larger than 48 W as shown in Table 2.

The temperature oscillation is weak at charging ratio 50 vol.%, the amplitude and periods become larger and longer with the increase of charging ratio, it is fierce at charging ratio 70 vol.%, sometime the amplitude of temperature oscillation beyond 10°C. The temperature oscillation is weakened with the increase of tilt angle as shown in Table 2.

3.4 Performance tests of mLHP at power cycles

The mLHP is operated under different heat load cycles to validate its operational reliability and transient response to the changing heat loads. In these tests, the heat load is varied in fixed step 12 W (heat flux density 1 W/cm^2) from 12 to 120 W. The performance tests at different charging ratios and tilt angles are shown in Fig. 5.

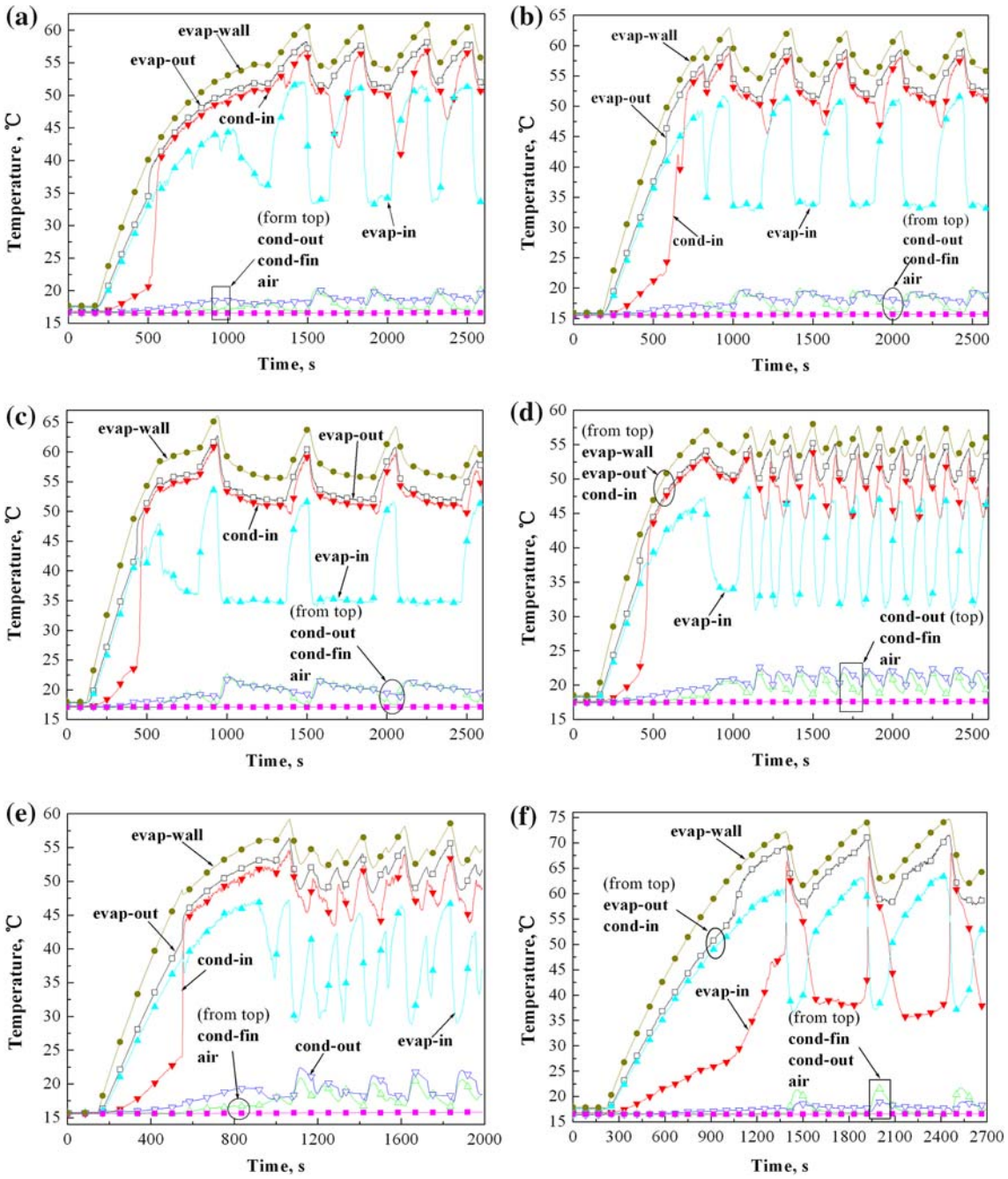

Fig. 4 Temperature oscillation of mLHP. **a** $\theta = 10°$, 60 vol.%, $Q = 24$ W. **b** $\theta = 10°$, 60 vol.%, $Q = 30$ W. **c** $\theta = 10°$, 60 vol.%, $Q = 36$ W. **d** $\theta = 50°$, 60 vol.%, $Q = 30$ W. **e** $\theta = 90°$, 60 vol.%, $Q = 30$ W. **f** $\theta = 10°$, 70 vol.%, $Q = 24$ W

It can be observed that for all the tested heat profiles the mLHP performed very efficiently and presented very fast response to the step changes in heat loads. For each run, the steady state is achieved within short transient period of 2–3 min following the change in the input heat load.

Comparing with the temperature oscillation when the heat load decreases from high-heat-load steady zone (III-zone) to the mid-heat-load oscillation zone (II-zone), the temperature oscillation is fiercer than that of the heat load increases from low-heat-load steady zone (I-zone) to the mid-heat-load oscillation zone. When the heat load increase from I-zone to II-zone, the liquid is charging into the compensation, the subcooled liquid cools the vapor and the evaporator wall, the power of the vapor decreases quickly. And when the heat load decrease from III-zone to II-zone, with the decrease of mass flow rate,

Table 2 Amplitude and periods of the temperature oscillations of $T_{evap\text{-}wall}$ at different operation conditions

Operation condition (W)		Amplitude (°C)	Periods (s)
$\theta = 10°$	18	4.05	320
60 vol.%	24	7.27	392
	30	8.08	415
	36	8.46	540
$\theta = 50°$	24	3.73	135
60 vol.%	30	4.93	148
	36	5.49	198
$\theta = 90°$	24	4.85	212
60 vol.%	30	6.03	210
	36	1.34	64
	42	1.65	75
$\theta = 10°$	24	2.81	605
50 vol.%	36	2.42	114
	48	1.32	55
$\theta = 50°$, 90° 50 vol.%		No obvious oscillation	
$\theta = 10°$	12	1.07	52
70 vol.%	24	12.54	540
$\theta = 50°$	12	7.82	258
70 vol.%	24	8.3	290
	36	11.1	520
$\theta = 90°$	24	6.32	218
70 vol.%	36	7.66	162

the bubble generates in the compensation chamber and decreases the subcooled liquid into the compensation chamber from condenser, meanwhile, the evaporator wall release heat capacity which quickens the bubble growing velocity and increases the quantity of bubble. The rate of bubble growth or dissipation inside the compensation chamber dictates the characteristics of the temperature oscillation.

As temperature oscillation occurrence, the temperature of evaporator wall reaches so high shown in Fig. 5c, even though the applied heat power is low. So sometimes the electronic device could invalidate at low heat load when the mLHP occurs temperature oscillation. It is significative to research the zone of temperature oscillation occurrence zone and the mechanism of the temperature oscillation of mLHP with flat evaporator.

4 Conclusions

In this paper, experimental investigation of the miniature loop heat pipe with flat evaporator, air cooling fin-tube condenser, and copper–stainless steel–methanol

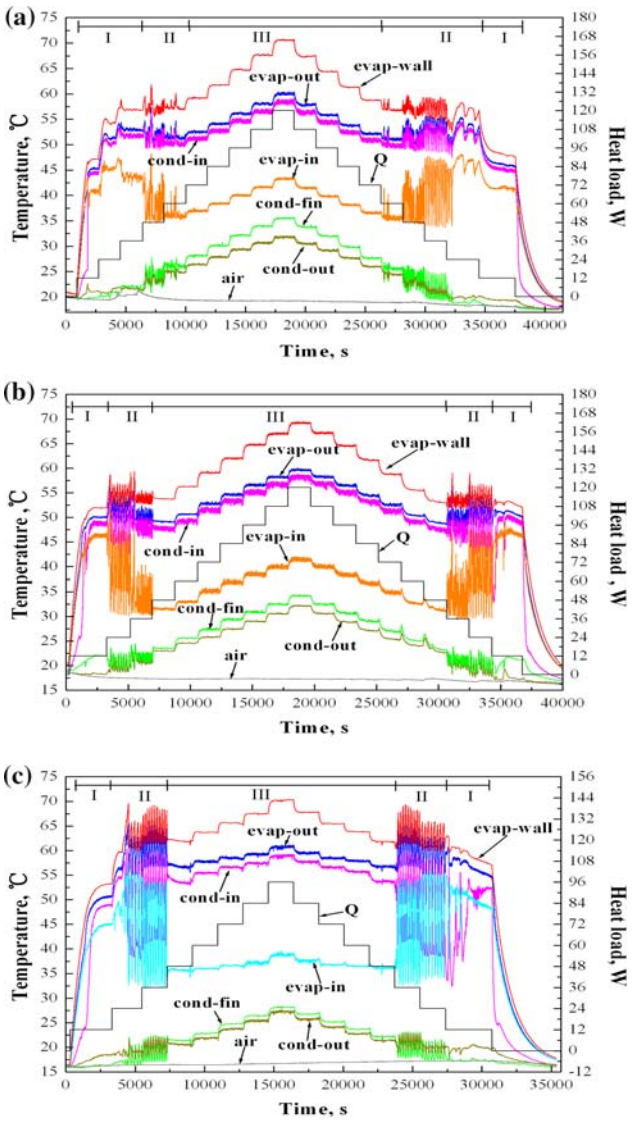

Fig. 5 Performance tests of the mLHP at power cycles. **a** $\theta = 10°$, 50 vol.%. **b** $\theta = 90°$, 60 vol.%. **c** $\theta = 90°$, 70 vol.%

configuration is conducted. The main outcomes of the study can be summarized as follows:

- The start-up time of mLHP increases with the decreases in the value of the applied heat load.
- The temperature of the mLHP increases with the charging ratio increasing, for the system needs larger superheat vapor to drive the loop, and it also increases the start-up time.
- With the tilt angle decrease, the temperature of the evaporator increases and the start-up time increases.
- The thermal resistance of the mLHP(R_{mLHP}) decreases with the increasing of the applied heat load.
- The R_{mLHP} decreases with the increase of the tilt angle.
- The R_{mLHP} increases with the increasing of charging ratio.

- Temperature oscillations are observed throughout the loop at some low heat load., it disappear when the heat load is larger than 48 W.
- With the increase of the charging ratio, the temperature oscillation becomes fiercer.
- With the increase of the tilt angle, the temperature oscillation is weakened.
- The compensation chamber is the most critical component of the mLHP, the rate of the bubble growth or dissipation inside the compensation chamber dictates the nature of the temperature oscillation.

Acknowledgments This research is supported by the National Natural Science Foundation of China (No. 50876035).

Appendix

See Figs. 1–5, Tables 1 and 2.

References

1. Maydanik YF (2005) Loop heat pipes. Appl Therm Eng 25(6):635–657
2. Stephane L, Valerie S, Bonjour J (2007) Parametric analysis of loop heat pipe operation: a literature review. Int J Therm Sci 46:621–636
3. Liu ZC, Liu W, Nakayama A (2007) Flow and heat transfer analysis in porous wick of CPL evaporator based on field synergy principle. Heat Mass Transf 43:1273–1281
4. Cheung KH, Hoang TT, Ku J, Kaya T (1998) Thermal performance and operational characteristics of loop heat pipe (NRL LHP). In: Proceedings of the 28th international conference on environmental systems, Danvers, MA, USA, SAE paper no. 981813
5. Ku J, Ottenstein L, Kobel M, Rogers P, Kaya T (2001) Temperature oscillations in loop heat pipe operation. AIP Conf Proc 552(1):255–262
6. Singh R (2006) Thermal control of high powered desktop and laptop microprocessors using two-phase and single phase loop cooling systems. PhD Dissertation. RMIT University, Australia
7. Vershinin SV, Maydanik Yu F (2007) Investigation of pulsations of the operating temperature in a miniature loop heat pipe. Int J Heat Mass Transf 50:5232–5240
8. Randeep S, Aliakbar A, Masataka M (2008) Operational characteristics of a miniature loop heat pipe with flat evaporator. Int J Therm Sci 47:1504–1515
9. Chen YM, Manfred G, Rainer M, Maydanik Yu F, Vershinin SV (2006) Steady-state and transient performance of a miniature loop heat pipe. Int J Therm Sci 45:1084–1090
10. Wukchul J, Yu T, Lee J (2008) Experimental study on the loop heat pipe with a planar bifacial wick structure. Int J Heat Mass Transf 51:1573–1581
11. Lee WH, Park KH, Lee KJ (2004) Study on working characteristics of loop heat pipe using a sintered metal wick. In: 13th IHPC, Shanghai, China, 21–25 September, pp 265–269
12. Boo JH, Chung WB (2004) Thermal performance of a small-scale loop heat pipe with PP wick. In: 13th IHPC. Shanghai, China, 21–25 September, pp 259–264
13. Roger RR, Thiago D (2005) Development of an experimental loop heat pipe for application in future space missions. Appl Therm Eng 25:101–112